www.geo-gsnl.org

Report template
version 1.6, 3/21

Biennial report for Permanent Supersite/Natural Laboratory

China Earthquake Supersite

History	China Earthquake Supersite – GSNL (geo-gsnl.org)
Supersite Coordinator	Yun Shao; Aerospace Information Research Institute, Chinese Academy of Sciences; No.9 Dengzhuang South Road, Haidian District, Beijing,China.

1. Abstract

China is one of the countries with the highest earthquake hazard in the world. This Supersite mainly has three scientific objectives (Figure 1) and one data sharing objective: 1) Postseismic deformation of the 2008 Wenchuan Mw7.9 earthquake. Acquire Sentinel-1 imageries of the 2008 Wenchuan Mw7.9 earthquake region in order to better resolve post-seismic deformation and understand how it affects nearby faults. 2) Interseismic deformation of the Haiyuan fault. Acquire high-resolution Cosmo-Skymed imageries of a selected section of the Haiyuan fault to study the interseismic deformation and aseismic creep. 3) Support the China Seismic Experimental Site (CSES). Acquire Sentinel-1 imageries at CSES sites to map the inter-seismic deformation and develop a high resolution structural model for the active faults by joint analysis of InSAR with other in-situ observations. 4) Data sharing. Advance data sharing (e.g. GNSS, Seismic waveforms, etc) in China, and promote international collaboration and participation of China in the GSNL initiative.

Since 2020, We have used a high-performance server to process a large number of images of Sentinel-1 data. We have focused on a series of earthquakes with magnitudes greater than 7 in East Asia (Figture 2), including the 1920 Haiyuan Mw7.9 earthquake, the 1976 Tangshan Mw7.6 earthquake, the 2001 Kokoxili Mw7.8 earthquake, the 2008 Wenchuan Mw7.9 earthquake in China, and the 2013 Balochistan Mw7.7 earthquake in Pakistan, etc. The results show that 1) postseismic deformation of the 1976 Tangshan earthquake is seriously affected by human activi

ties, such as groundwater extraction, and it is difficult to obtain the postseismic deformation signals only through InSAR data. 2) There is a significant creep phenomenon in the Laohushan section of the Haiyuan fault, with a creep rate of about 5 mm/yr, while the research of spatiotemporal distribution of the aseismic creep and the seismic risk of the Haiyuan fault are underway. 3) The best estimated viscosities for the lower crust and upper mantle of the Kokoxili regions were 1 (+0.78/-0.44) x 10^{19} Pas and 1 (+0.78/-0) x 10^{20} Pas, respectively, and the obtained value was largely the same as the previously estimated steady-state viscosity. 4) There is obvious decorrelation due to the complex terrain and dense vegetation in the 2008 Wenchuan Mw7.9 earthquake area. 5) Surface displacements of the 2013 Balochistan Mw7.7 earthquake were caused by ∼ 80 cm of aseismic slip along a 5,500-km 2-wide subhorizontal patch of the megathrust fault, corresponding moment is Mw 7.3. Our results will contribute to understand mechanism of earthquake occurence and benefit to evaluate seismic hazard.

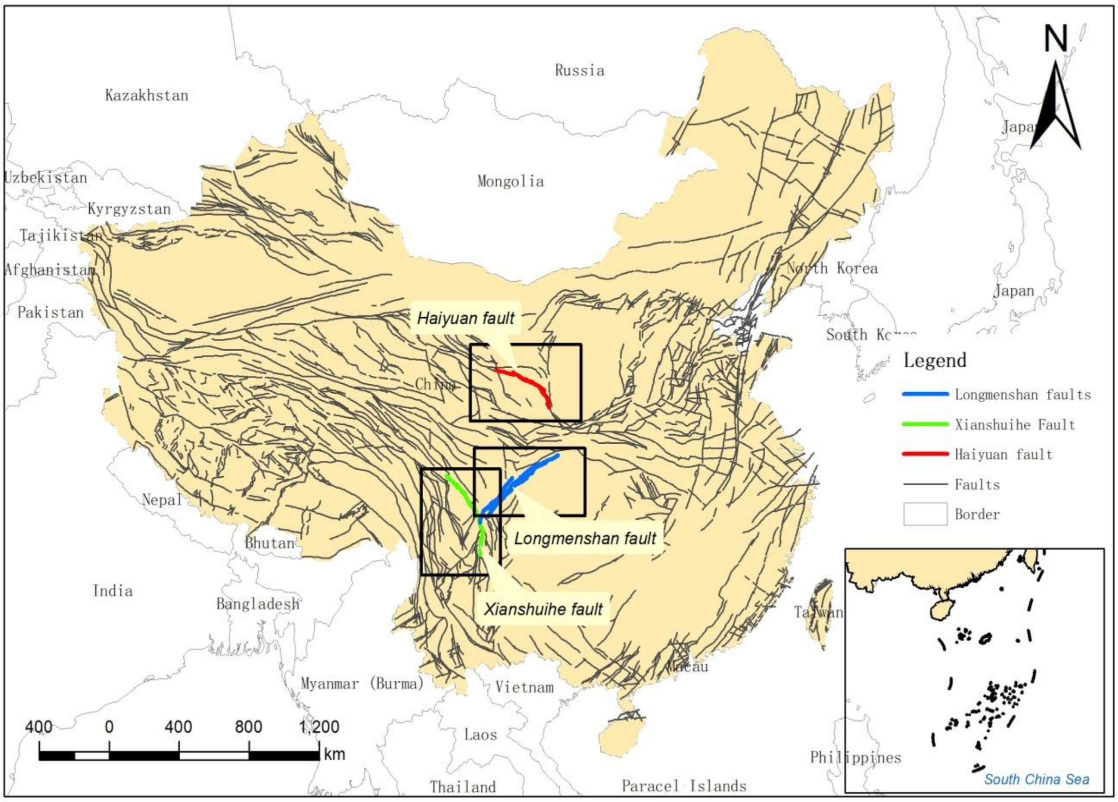

Figure 1. Objectives of China Earthquake Supersite

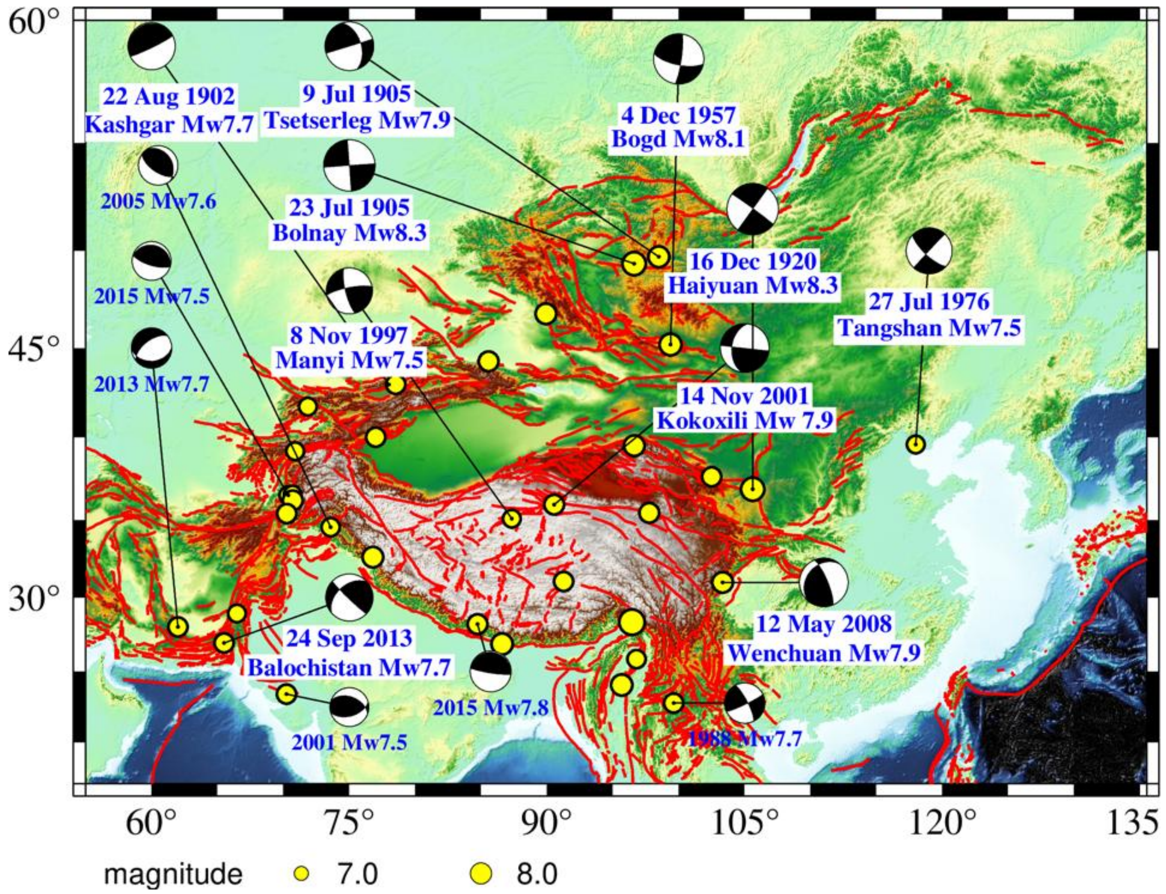

Figure 2. main earthquake (larger than M7) in east Asia since 1900

2. Scientists/science teams

Name:	Yun
Surname:	Shao
Position:	Professor
Email:	Shaoyun@radi.ac.cn
Personal web page:	http://sourcedb.radi.cas.cn/zw/zjrck/yjy/201304/t20130402_3812305.html
Institution:	Aerospace Information Research Institute, Chinese Academy of Sciences
Address:	No.9 Dengzhuang South Road, Haidian District, Beijing, China

Name:	Falk
Surname:	Amelung

Position:	Professor
Email:	famelung@rsmas.miami.edu
Personal web page:	https://people.miami.edu/profile/f.amelung@miami.edu
Institution:	University of Miami
Address:	Coral Gables, Miami, Florida, USA
City:	Miami

Name:	Xiaoyong
Surname:	Wu
Position:	PhD student
Email:	xywu@aircas.ac.cn
Institution:	Aerospace Information Research Institute, Chinese Academy of Sciences
Address:	No.9 Dengzhuang South Road, Haidian District, Beijing, China

Name:	Xiaoran
Surname:	Lv
Position:	PhD student
Email:	lvxr@radi.ac.cn
Institution:	Aerospace Information Research Institute, Chinese Academy of Sciences
Address:	No.9 Dengzhuang South Road, Haidian District, Beijing, China

Name:	Shu
Surname:	Ye
Position:	PhD student
Email:	2818536595@qq.com
Institution:	Aerospace Information Research Institute, Chinese Academy of Sciences
Address:	No.9 Dengzhuang South Road, Haidian District, Beijing, China

Name:	Xiaoqing
Surname:	Wang
Email:	wangxiaoq517@163.com
Position:	Researcher
Institution:	Institute of earthquake science, China Earthquake Administration
Personal web page:	http://www.seis.ac.cn/manage/html/8a9080a125b29b1b0125b2a3093a0002/_content/10_06/25/1277430254101.html
Street address:	No 63, Fuxing Street, Haidian District, Beijing,China

Name:	Guosheng
Surname:	Qu
Email:	qgsh@263.net
Institution:	National Earthquake Response Support Service (NERSS),Ministry of Emergency Management
Position:	Full Prof. Director of S&T, National Earthquake Response Support Service (NERSS), Ministry of Emergency Management; Vice President of The International Emergency Management Society (TIEMS) ; Experts Group Leader of China Earthquake SAR; Deputy General Team Leader of China International SAR Team (CISAR); General Coach of China USAR (CSAR); Classifier for IEC/IER of UNOCHA; Expert of Fire Fighting Bureau of Ministry of Emergency Management
Address:	No.1, West Yuquan Street, Shijingshan, Beijing, China

Name:	Ming
Surname:	Liu
Email:	euler@dasa.net.cn
Institution:	Laboratory of Target Microwave Properties, Deqing Academy of Satellite Applications
Position:	General engineer

Address:	Geographic information town, Deqing county, Zhejiang Province, China

Scientists/science teams issues

The research work mainly encounters the following issues:

1) The research work has a long way to go. The research work is mainly completed by three students under the guidance of the professor Shao and professor Amelung. It is difficult to solve many outstanding scientific problems at the same time in a short time. In addition, it is hard to collect in-situ data (e.g. GNSS, seismic waveforms) given that the data protection and strict management.

Solution: In term of in-situ data collecting, Professor Wang and Professor Qu, Who have worked in China Earthquake Administration for many years, have incorporated into our team. They can help us communicate and coordinate with the relevant departments of the China Earthquake Administration.

2) Estimation and inversion Geophysical parameters. It is well known that estimation and inversion of geophysical parameters are difficult and time-consuming. To obtain the model parameters that best fit the observation data, it is very dependent on data precision, methods, especially our knowledge and experience.

Solution: We have purchased a high-performance server in order to improve computing efficiency. In term of estimation and inversion Geophysical parameters, we not only constantly try and error but also adopting new method (e.g. Bayesian) to improve the accuracy and precise of results.

1. In situ data

Type of data	Data provider	How to access	Type of access
GPS time series	China Earthquake Network Center	The CEA operates a network of 260 continuous GNSS stations and 2000 regional stations. The data for continuous and regional GNSS data are available on request:	registered public

		https://www.cenc.ac.cn/	
GPS velocity	1)China Earthquake Network Center, 2)Published Articles	1)The data for GNSS velocity are available on request: https://www.cenc.ac.cn/ 2)In the past few decades, a large number of articles about surface deformation have been published, and these articles often accompanied by processed GPS velocity field data.	1)registered public 2)unregistered public
Seismic events	China Earthquake Network Center	Seismic events are available from: http://www.ceic.ac.cn/	unregistered public
Seismic waveforms	China Earthquake Network Center	The seismic Network Data Backup Center archives the seismic waveforms: https://data.earthquake.cn/index.html	registered public

In situ data issues

1) Data accessibility. The in-situ data (e.g. GNSS, seismic waveforms etc) operated and maintain ed by various departments of the China Earthquake Administration will eventually be archived i n the China Earthquake Networks Center. But most in-situ data are limited without cooperation given that data projection and strict management.

2) Reference frame of Published GNSS data. In the past few decades, many high-level articles re lated to seismic deformation and geological structure have been published. These articles are o ften accompanied by preprocessed data, such as GNSS time series and velocity field. However, s ince the reference frame used by each research is not always the same, it is necessary to conver t each data set into a unified reference frame when using it.

2. Satellite data

Type of data	Data provider	How to access	Type of access
Sentinel1	ESA and ASF	The data for Sentinel1 can be accessed in ESA: https://scihub.copernicus.eu/dhus/#/home or ASF: https://search.asf.alaska.edu/	registered public

COSMO-SkyMed	ASI	The data for COSMO-SkyMed can be applied for GSNL.	limited to GSNL scientists

Satellite data issues

1) Data push. We ordered more than 100 COSMO-SkyMed images from GSNL, and GSNL pushed 4 images to us through ftp every other time, which has lasted for nearly two years. We need to wait for most of the images to be received before conducting time series analysis. At present, we only use the sentinel-1 images.

3. Research results

From 2020 to present, we have used the high-performance server of Texas Advanced Com puting Center to process a large number of images of Sentinel-1 data. We have focused on a ser ies of earthquakes with magnitudes greater than 7 in East Asia (Figture 3), including the 1902 K ashgar Mw 7.7 earthquake, the 1920 Haiyuan Mw7.9 earthquake, the 1976 Tangshan Mw7.6 ea rthquake, the 2001 Kokoxili Mw7.8 earthquake, the 2008 Wenchuan Mw7.9 earthquake in Chin a; and the 1905 Bolnay-Tsetserle Mw8.5 earthquake and the 1921 Bogd Mw 8.1 earthquake in Outer Mongolia; and the 2013 Balochistan Mw7.7 earthquake in Pakistan, etc.

The Interferometric Wide swath (IW) mode of Sentinel-1 was used in this study. Interferog rams with seven looks in the azimuth direction and 21 looks in the range direction were constru cted using the JPL/Caltech ISCE stack processor (Fattahi et al., 2017, Rosen et al., 2012). For eac h epoch, we generated interferograms using itself and the next five epochs following it. The 30 m Shuttle Radar Topography Mission (SRTM) digital elevation model and the Precise Orbit data were used to simulate and remove the topographic phases and flatten earth phases from each i nterferogram. By finding the offsets between the master SLC (Single Look Complex) and SLCs us ing the DEM and orbit vectors, multi-looked and filtered interferograms were co-registered to a single master SAR image. Finally, the statistical-cost network-flow algorithm (SNAPHU) was use d to unwrap the phases of the co-registered interferograms. Based on these steps, we obtained a stack of phase unwrapped interferograms co-registered to a common SAR acquisition, correc ted for earth curvature and topography.

The open-source Miami InSAR time-series software in Python (MintPy) is used for time-series processing (Yunjun et al.,2019). MintPy uses distributed scatterers and is an improved small baseline subsets (SBAS) algorithm, which uses a fully connected network of interferograms and performs phase corrections in the time-series domain, in contrast to the conventional interferogram domain. Based on the routine processing workflow of MintPy, the raw phase time-series was first inverted from the interferogram network (known as phase triangulation). Subsequently, the solid earthquake tide phase, topographic residuals, and tropospheric delay using the global atmospheric models (ERA5 from the ECMWF) were calculated and removed from the raw phase time-series. Finally, the average line-of-sight (LOS) velocity was estimated on a pixel-by-pixel basis using the noise-reduced displacement time series.

For each pixel, the deformation is a relative measurement with respect to a reference pixel on the same track. Thus, when the deformation velocity fields of adjacent tracks are concatenated, a constant offset, which is the median of the differences in the deformation velocity fields in the overlapping areas, is first estimated. Subsequently, the average deformation velocity of the two tracks for the overlapping areas is used.

Finally, the ascending and descending data are combined to vertical and east-west deformation velocity components, assuming that the ascending images are acquired on the same day as the descending images, although they are acquired four days later. Ascending data with linear ramps removed are presented throughout the paper.

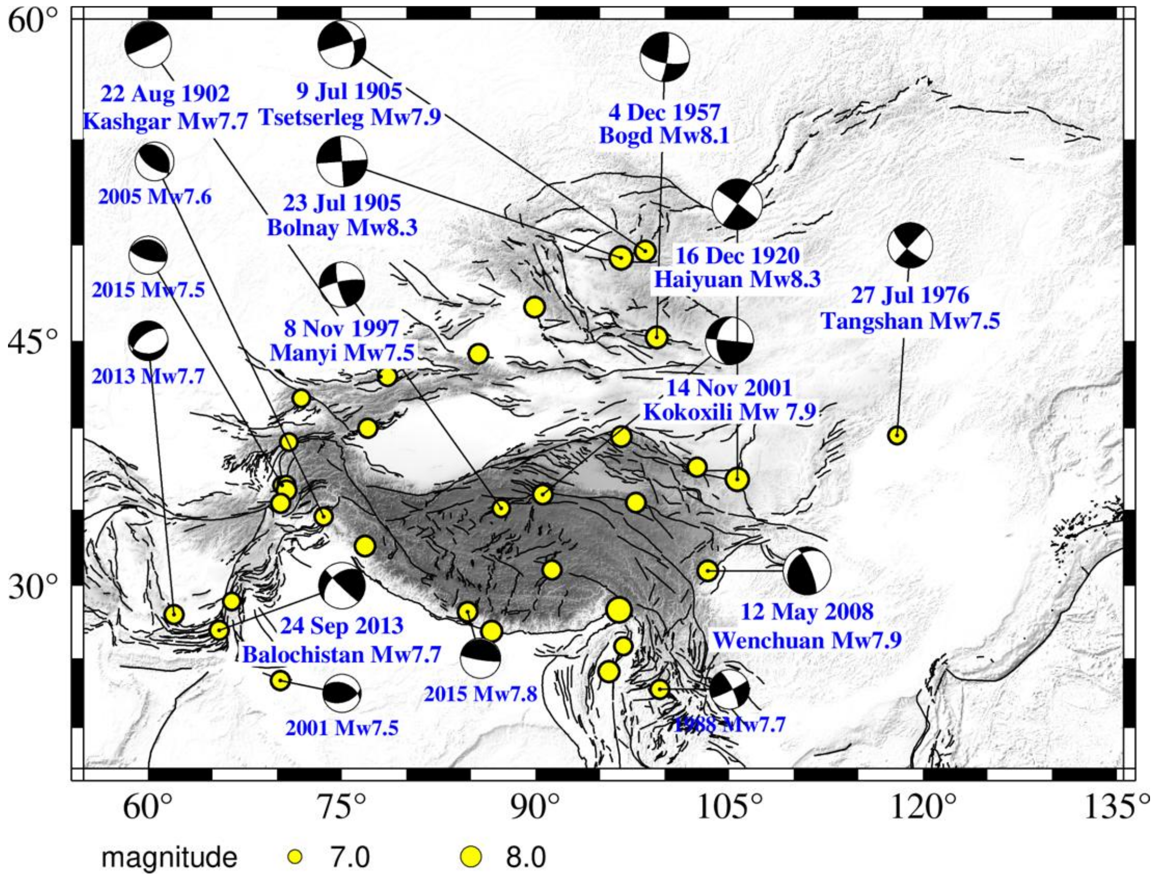

Figure 3. Main earthquakes with magnitude larger than 7 in East Asia since 1900

(1)The 1976 Tangshan Mw7.6 earthquake

The deformation rate shows that there is obvious subside signal in the earthquake area (Fig.3), which may be affected by human activities, such as groundwater extraction. But it is difficult to obtain the postseismic or interseismic deformation signals in the earthquake area only through InSAR data.

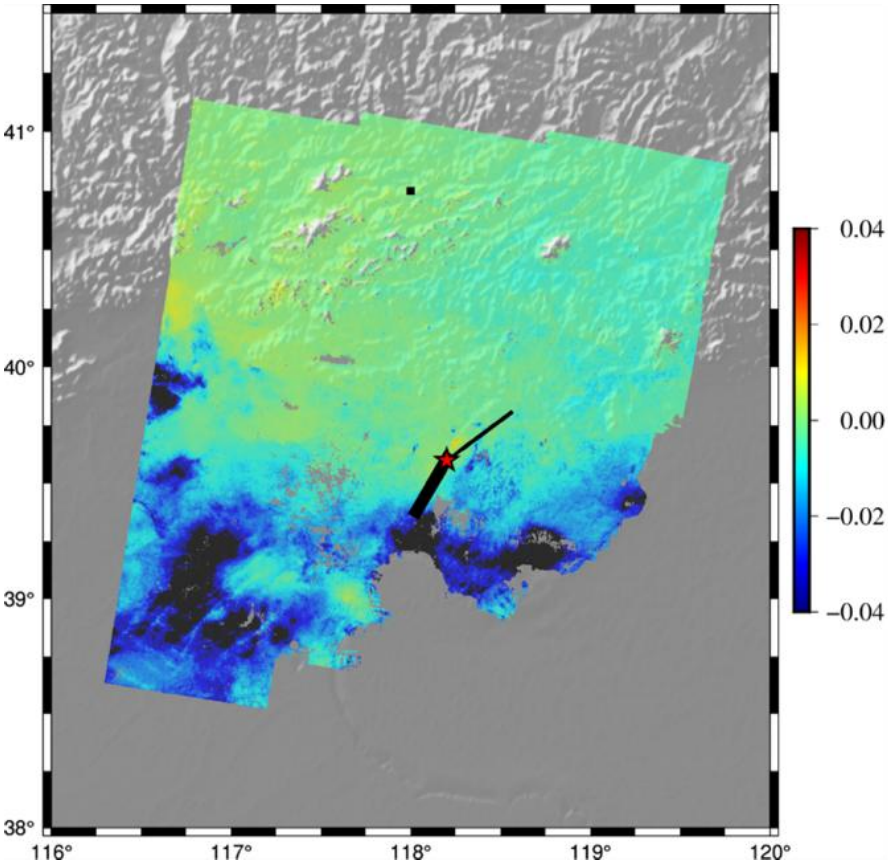

Figure 4. InSAR LOS velocity in Tangshan.

the black rectangle and the red star is seimogenic fault and epicenter of the 1976 Tangshan Mw7.6 ea rthquake, respectively.

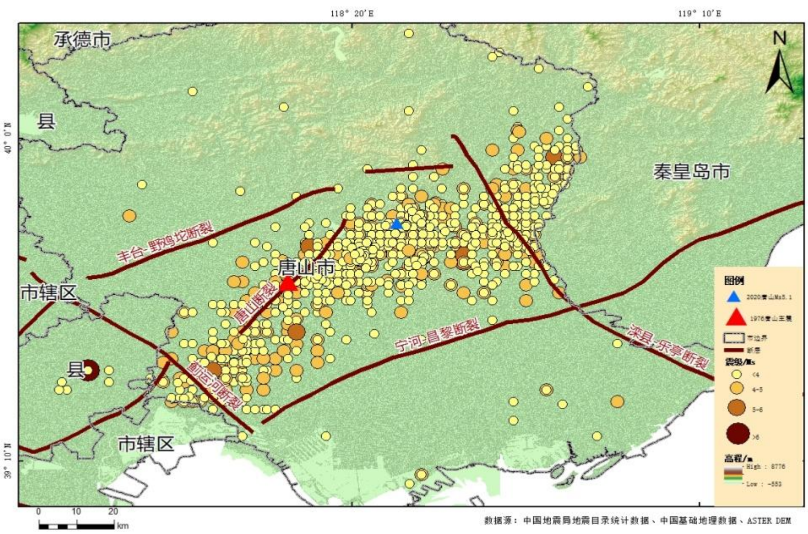

Figure 5. Epicenter distribution map after the 1976 mainshock.

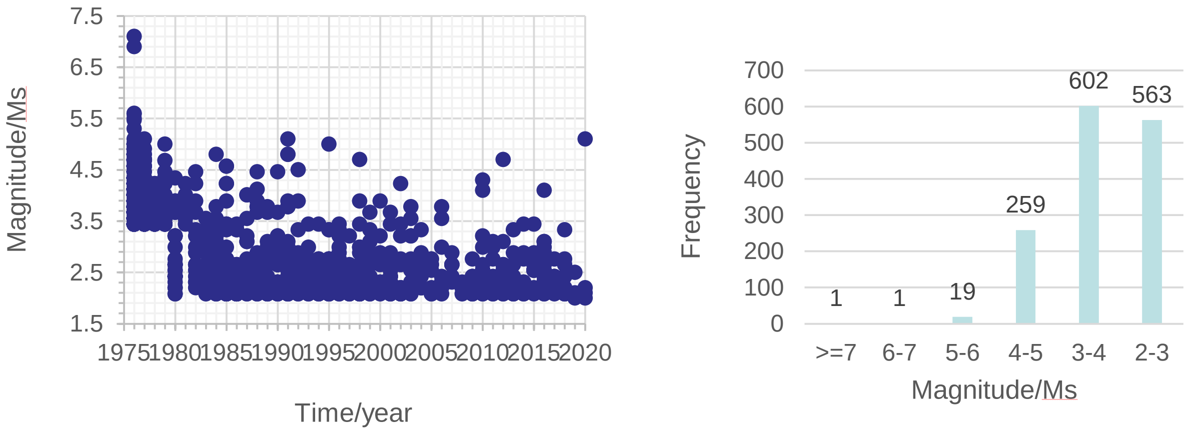

Figure 6. Statistics on the magnitude and frequency after 1976 Tangshan mainshock.

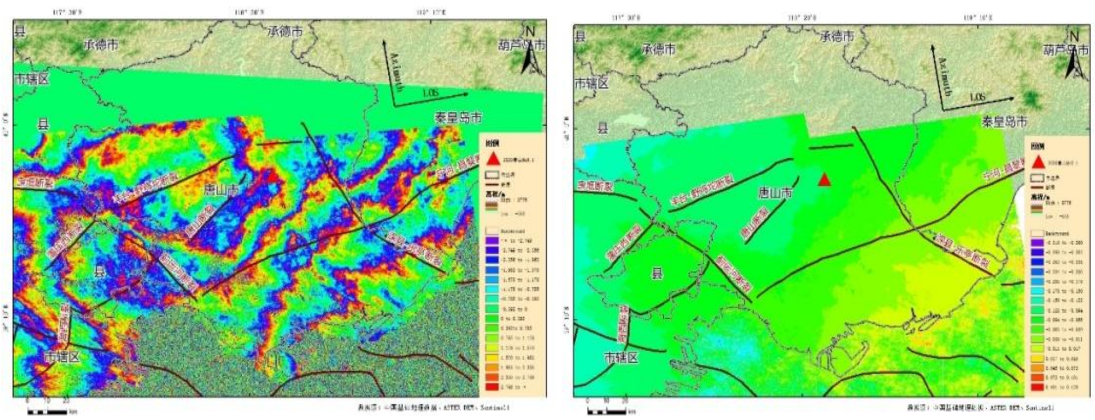

Figure 7. InSAR interferogram and coseismic deformation of the Tangshan M5.1 earthquake on July 12, 2020

(2)The 2001 Kokoxili Mw7.8 earthquake

Time-series observations from Sentinel-1 A/B InSAR spanning November 2014 to July 2021 were used to study the late post-seismic deformation velocity field arising from the Kokoxili ear thquake. The deformation velocity caused by the interseismic slip along the major active faults i n Tibet was first simulated. Comparing the simulated deformation velocity with the observed o ne, the maximum ratio of the simulated deformation velocity to the observed one was found to be 42%, indicating continuity in the viscoelastic relaxation caused by the 2001 Kokoxili earthqu ake. Subsequently, the rheological structure of the Kokoxili region was explored using a mixed model comprising the viscoelastic relaxation mechanism and the buried elastic dislocation mod el. The best estimated viscosities for the lower crust and upper mantle were 1 (+0.78/-0.44) x 1

0^{19} Pas and 1 (+0.78/-0) x 10^{20} Pas, respectively. The results obtained in this study were compared with those of previous studies that used the early post-seismic displacement ranging from 0 to 6.5 years following the earthquake. The obtained value was largely the same as the previously estimated steady-state viscosity, which means that the viscosities of the viscoelastic layer beneath the Kokoxili regions have almost reached their stable state. Furthermore, the effective lower crustal viscosity of the Kokoxili region exhibited a logarithmic trend with time. This work is mainly completed by Dr. Lv (Lv and Shao,2022).

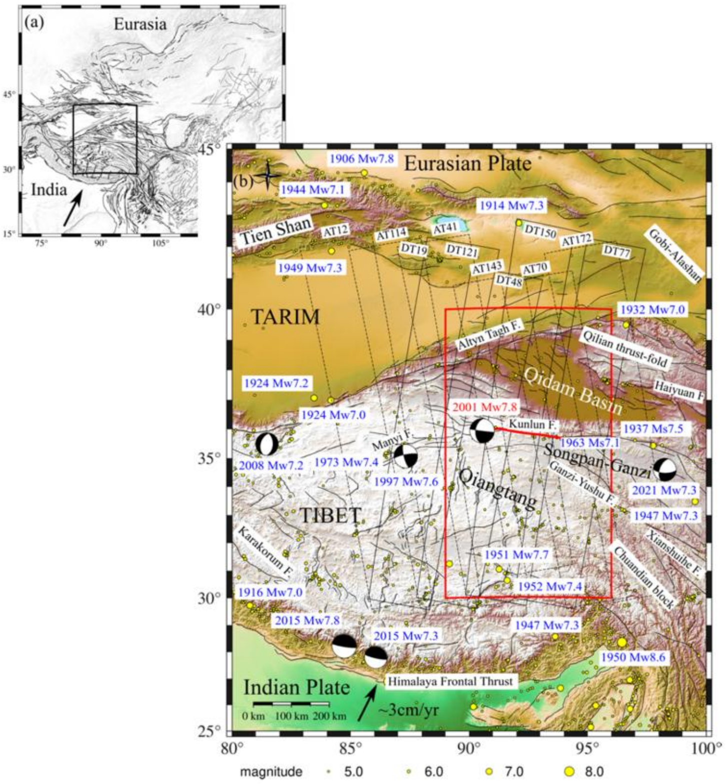

Figurte 8. (a) Location of study area in East Asia. The black thick solid rectangle represents the location of the study area. (b) Study area. The yellow circles are events with magnitudes greater than Mw 5.0. The black dashed rectangles and black solid rectangles are Sentinel-1 ascending and descending tracks, respectively. Red texts and the beach ball beneath them show the epicenter of the Kokoxili earthquake. Red solid line is the surface rupture, and red rectangles are the deformation area used for modeling. Black thin lines in (a,b) are faults.

table 1. the Sentinel-1 data of Hoh Xili earthquake

track	Span time	images
AT12	201411 - 202107	165

AT114	201411 - 202105	159
AT 41	201411 - 202107	163
AT 143	201411 - 202105	155
AT 70	201411 - 202107	158
AT172	201411 - 202107	161
DT19	201411 - 202107	161
DT121	201411 - 202107	158
DT 48	201411 – 202103	151
DT 150	201411 - 202105	154
DT 77	201411 - 202107	143

Figure 9 shows the LOS velocity field. It can be seen that for the ascending track data, there are large deformation areas on both sides of the fault. The deformation rate in the north of the faul t is as high as 7 mm/yr, and the deformation rate in the south of the fault is as high as 10 mm/y r. For the decending track data, the deformation area in the north of the fault presents a narro w and long rectangle, and the maximum deformation rate is 8 mm/yr; There are two discrete d eformation regions in the south of the fault, with the maximum deformation rate of 6 mm/yr.

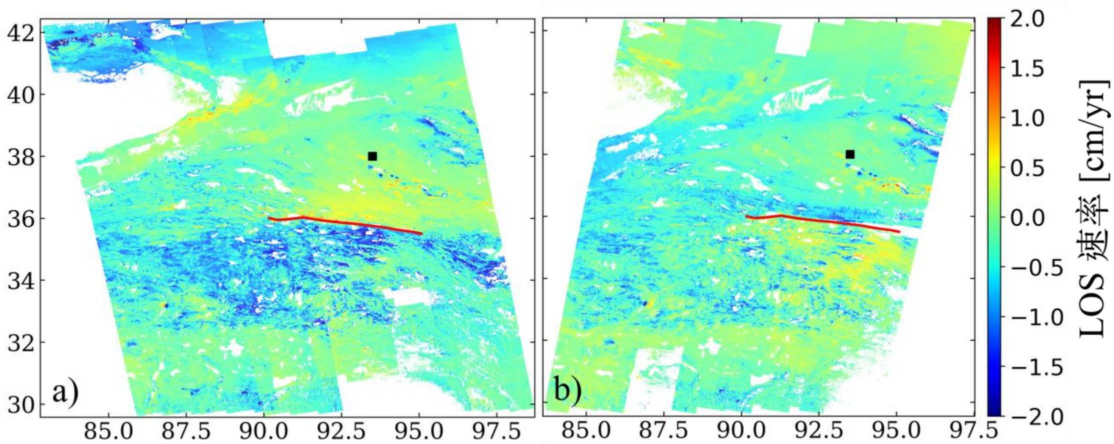

Figure 9. (a,b) Observed LOS post-seismic deformation velocities for the ascending and descending orbits, res pectively. Black dot: reference point. Red lines are surface rupture of the Kokoxili earthquake.

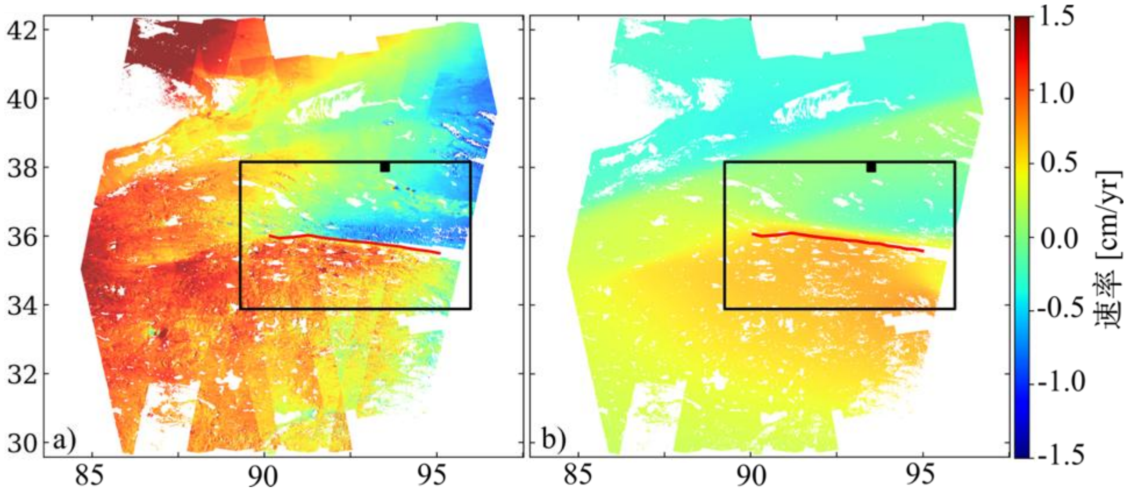

Figure 10. (a) Observed east−west deformation velocity and (b) simulated east−west deformation velocity. Black dot: reference point. Red lines are surface ruptures of the Kokoxili earthquake. The black rectangle: spatial region with latitude ranging from 34° N—38° N and longitude ranging from 87° E—96° E.

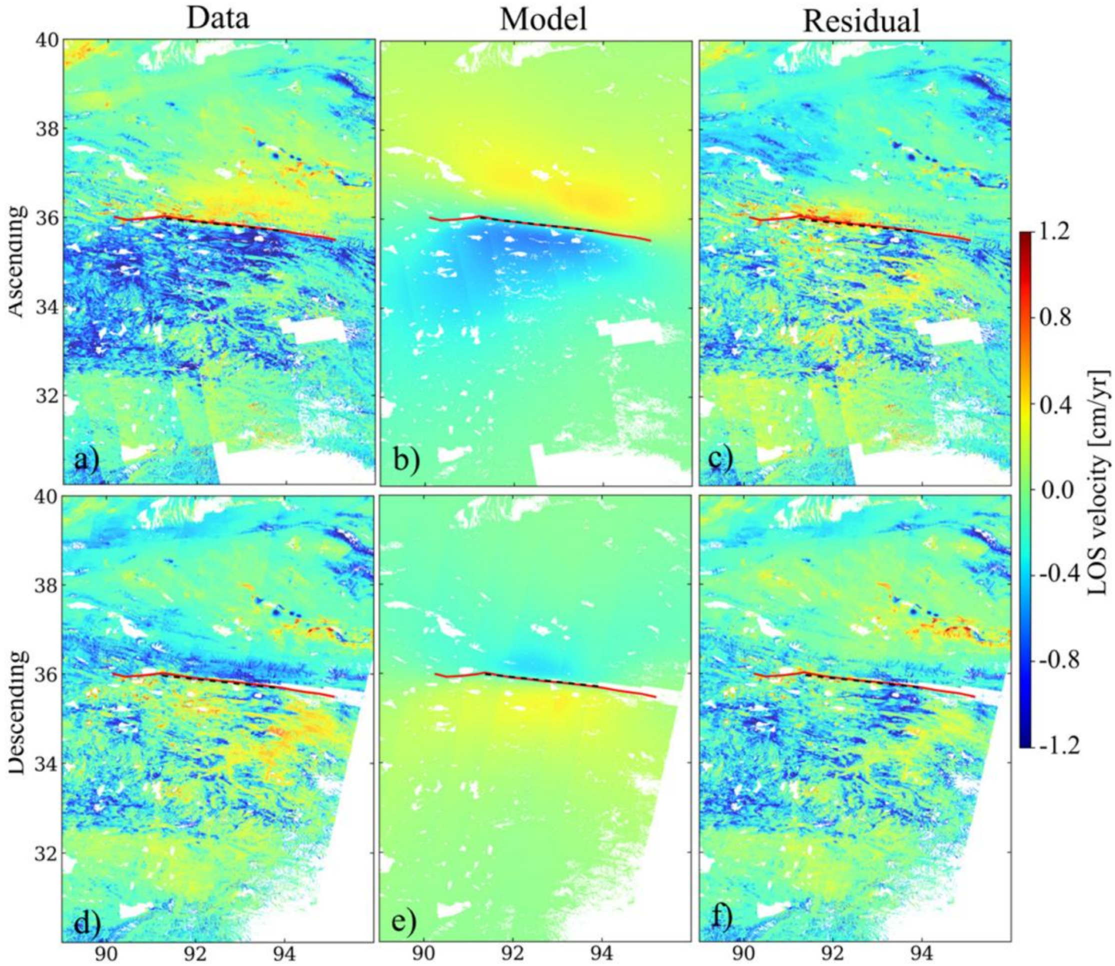

Figure 11. Best−fitting modeling results for the mixed model for concatenated ascending and descending tracks. The red solid line marks the coseismic fault. The black dashed line marks the surface project of the best fitting buried elastic dislocation. (a,d) are observation for ascending and descending, respectively. (b,e) are the model results for ascending and descending, respectively. (c,f) are residual for ascending and descending, respectively.

(3)The 2008 Wenchuan Mw7.9 earthquake

Acquire Sentinel-1 imageries of the 2008 Wenchuan Mw7.9 earthquake region in order to better resolve post-seismic deformation and understand how it affects nearby faults.

It can be seen from the Figure 12 that: 1) There is obvious decorrelation due to the comple x terrain and dense vegetation in the earthquake area, so only the deformation signal in the sou theast direction of the fault can be obtained. 2) There are still obvious post-earthquake deform ation signals between 2014 and 2020.

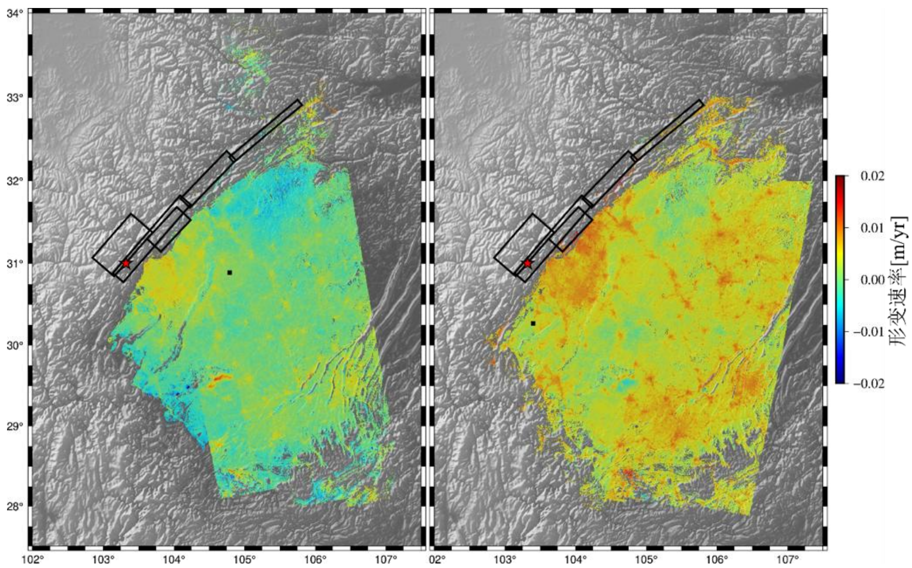

Figure 12. 2014-2021 Postseismic deformation LOS velocity（a）ascending track（b）decending track. The red star is epicentre, and the black rectangle is seimogenic fault.

(4)The 1920 Haiyuan Mw7.9 earthquake and interseismic deformation

In the past 70-50 million years (Ma), the convergence of the Indian and Eurasian plates has created the youngest and most magnificent continental collision zone on Earth, namely the Hi malayan-Tibet orogenic belt (Molnar and Tapponnier, 1975; Yin and Harrison,2000). Earthquakes occur frequently on the Tibet Plateau and its surrounding areas, as well as in East Asia.

The relationship between aseismic sliding and tectonic loading is crucial for understanding the strain accumulation pattern along faults and the ability to generate large earthquakes. Whether aseismic creep is continuous or episodic in time has important implications for seismic hazard as episodic creep could trigger larger events. This chapter utilized time-series InSAR and GPS data to investigate the spatial distribution and temporal evolution of aseismic creep along the Laohushan section of the Haiyuan Fault. The discontinuity of the cross fault velocity field indicates that the fault creep ruptured to the surface, with a velocity parallel to the fault strike of 5mm/yr.

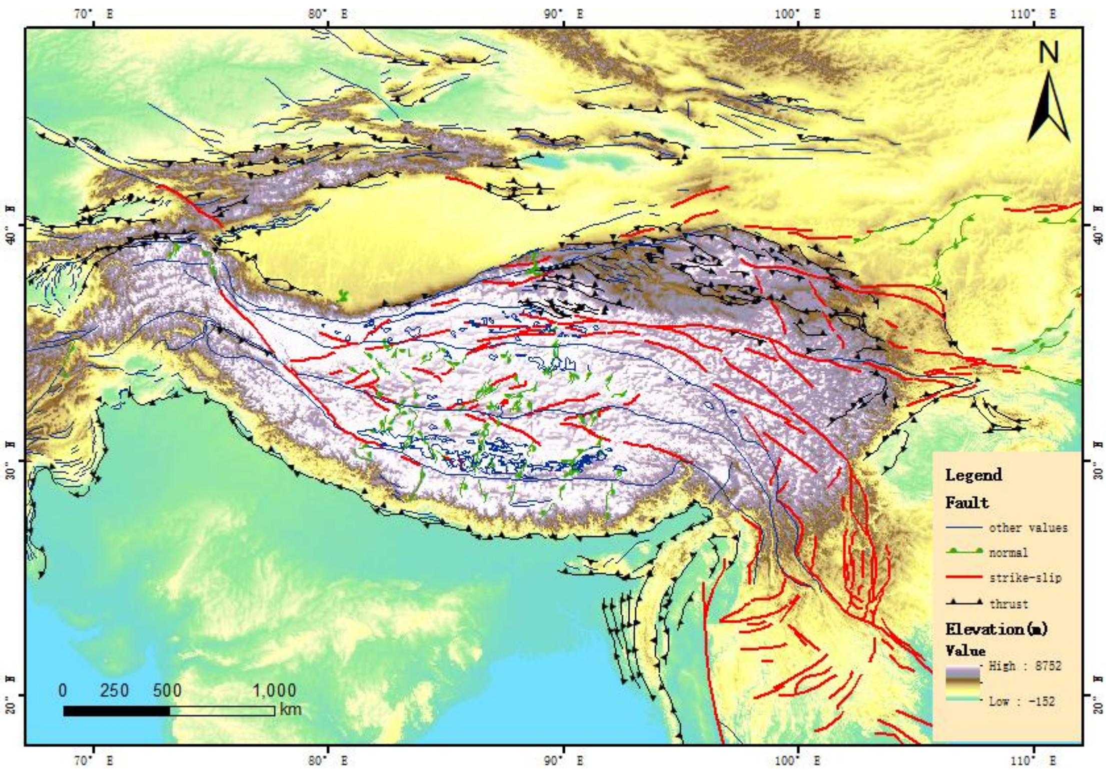

Figure 13. Topography and main structure (modified according to Taylor and Yin (2009))

GPS time series

The GPS coordinate time series records the change of the coordinate position of GPS stations, as shown in Figure 14 and Figure 15, which are the GPS coordinate time series of continuous stations and compaign stations, respectively. It can be seen from Figure 14 and Figure 15 that t he overall movement of GPS stations is relatively slow and uniform, reflecting the stability of te ctonic activity. But it is difficult to use GPS observation data alone to study the refined moveme nt characteristics of faults.

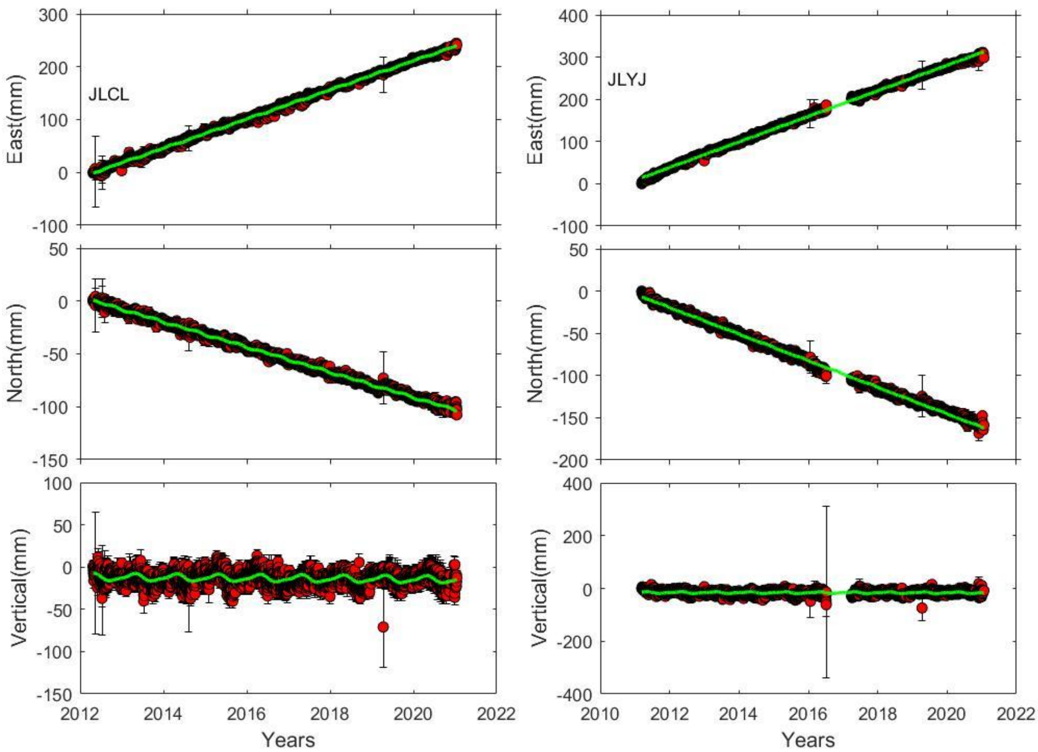

Figure 14. Time series of continuous GPS station

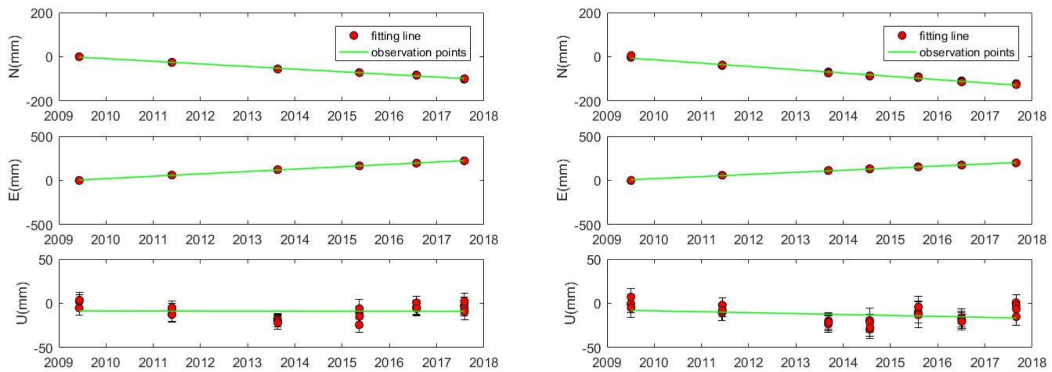

Figure 15. Time series of campaign GPS Station

GPS velocity

The GPS velocity field reflects the characteristics of tectonic movement. Usually, the satelli te observation signals are received by GPS stations, and the velocity field is calculated by fitting

GPS coordinate time series or using professional processing software such as GAMIT/GLOBK, Be nerse, Gipsy, et al. However, because the raw GPS observation data is sensitive and difficult to obtain, we collected the GPS coordinate time series data of the study area and obtained the vel ocity field through data fitting.

InSAR velocity

In this study, a total of 4 strips of Sentinel-1/IW images (Figure 16 and table 2) were used. Each strip spanned 3-4 years of continuous observation data (2014-2020), and the time interval between most images was 12 days, ensuring good time coherence.

table 2. the Sentinel-1 data of Haiyuan fault

Faults	Beam mode	Flight direction	Path	Frame	Acquisitions	Periods
Haiyuan	IW	Ascending	55	112	105	20140327-20201106
				117	105	20140327-20201106
			157	112	94	20140202-20201101
				117	94	20141012-20201101
		Decending	62	469	78	20140322-20201106
				472	40	20141009-20201125

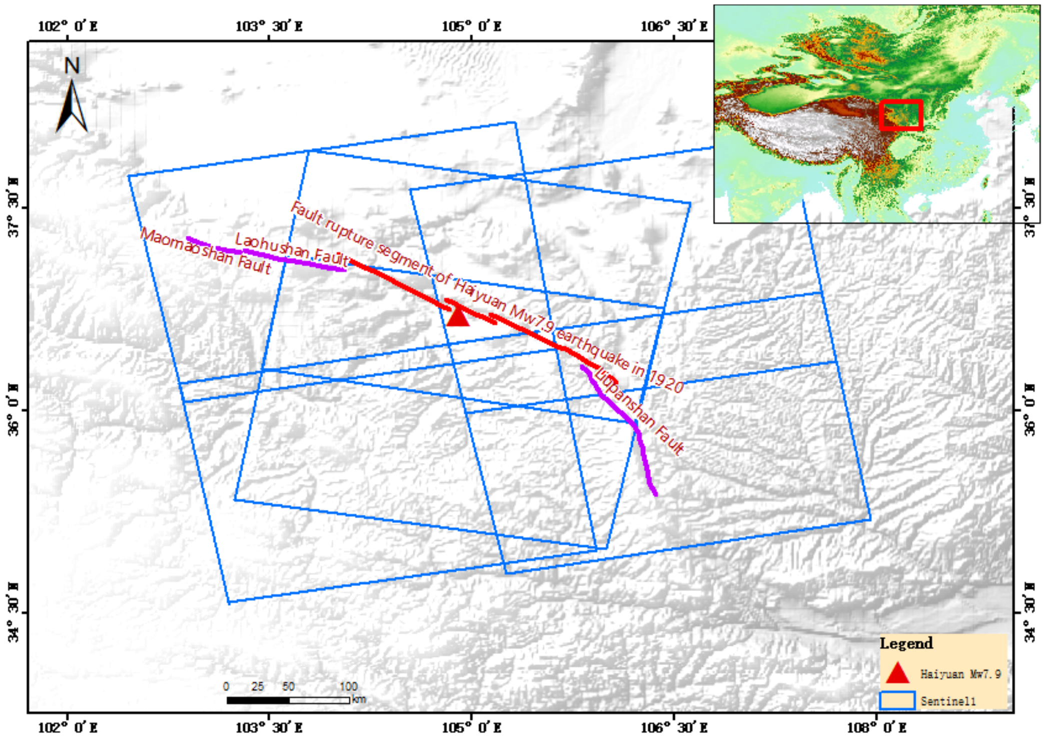

Figure 16. The coverage of sentinel1 images and GPS data

Figture 17 shows the deformation rate field in the Haiyuan earthquake area. It can be seen that there are obviously opposite deformation signals on both sides of the Haiyuan fault. It can be seen from Figture 18 and Figture 19 that the horizontal deformation presents obvious arctan gent curve characteristics along the profile perpendicular to the fault, which indicates that the Haiyuan fault is in the inter-earthquake sliding stage.

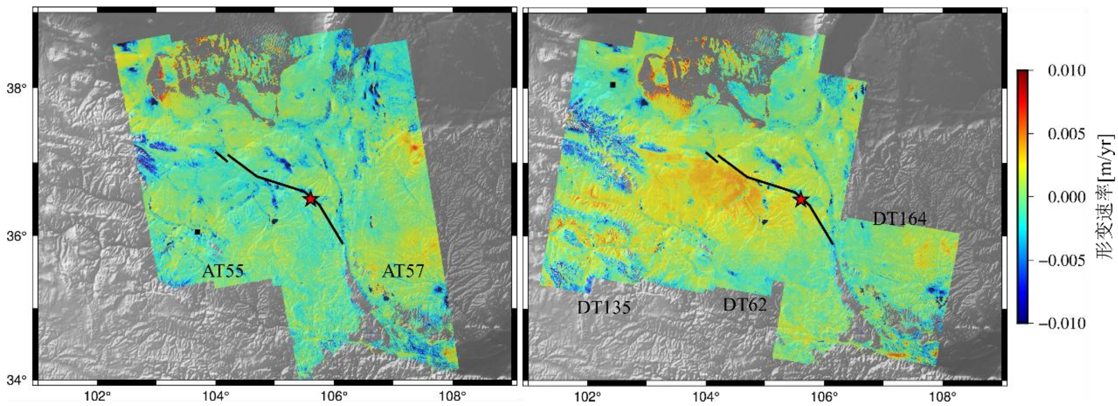

Figure 17. LOS deformation velocity in Haiyuan fault.The black line is seismogenic fault,and the red star is epicenter

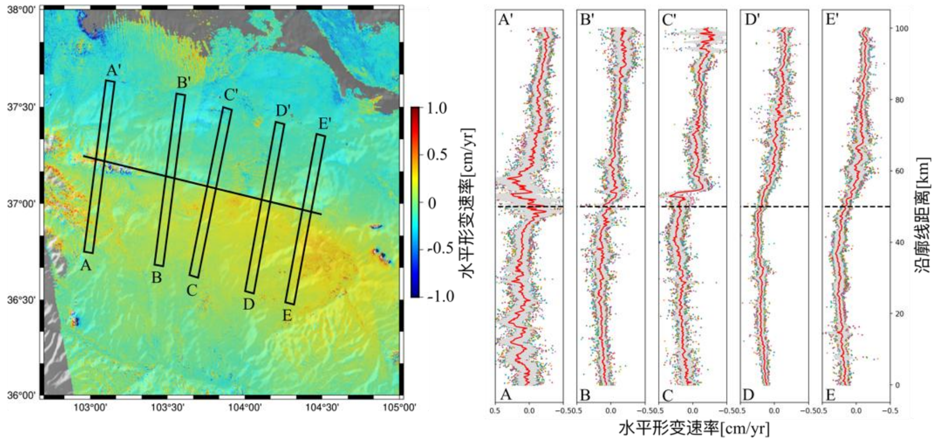

Figure 18. Horizontal deformation velocity.the balck line is Haiyuan fault.

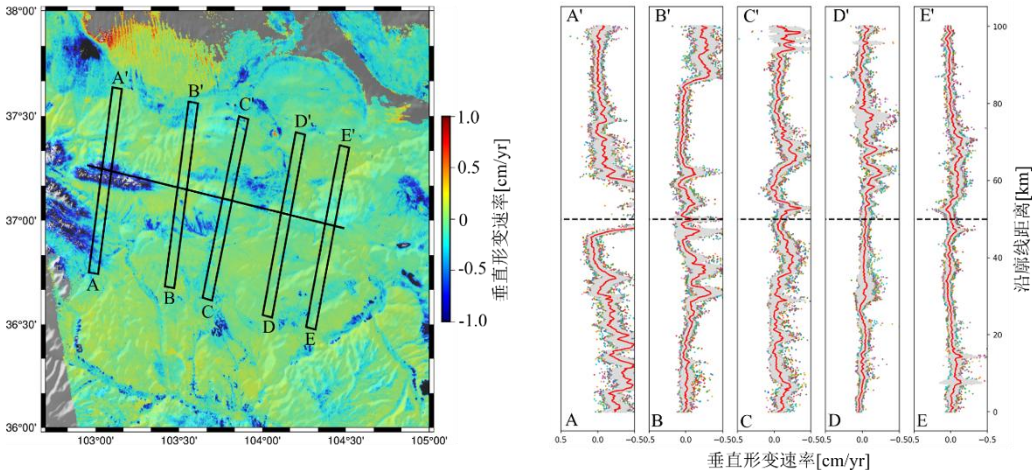

Figure 19. Perpendicular deformation velocity. And the balck line is Haiyuan fault.

Although there are few GPS stations, the addition of GPS data is a good supplement to the InSAR deformation results and provides better constraints for the inversion of interseismic defo rmation. At present, the overall tectonic movement of Haiyuan fault zone is relatively stable, an d creep phenomenon has been found in some areas (such as Tianzhu), and further research and analysis of seismic hazard is under way.

(5) The 2013 Balochistan Mw7.7 earthquake

InSAR time series data for the 2014 – 2021 period reveal up to 20 cm of radar line-of-sight displacements in the area of the 2013 Mw 7.7 Balochistan earthquake northwest of the Hoshab Fault in the eastern Makran subduction zone in southwest Pakistan. We show that surface displ acements were caused by ~80 cm of aseismic slip along a 5,500-km 2-wide subhorizontal patch of the megathrust fault. The corresponding moment is Mw 7.3. The percentage of slip in plate-perpendicular direction ranges from ~65% in the northwest to 96% in the southeast. Slip is consistent with shear stress imparted by the 2013 earthquake. The triggered aseismic slip suggests that this section of the megathrust is decoupled. The implication for the seismic potential of the subduction zone is that the megathrust is fully locked to at most 220 km distance from the trench, consistent with the lack of M ⩾ 9 earthquakes in the historic record. This work is mainly completed by Dr. Lv (Lv et al.,2022).

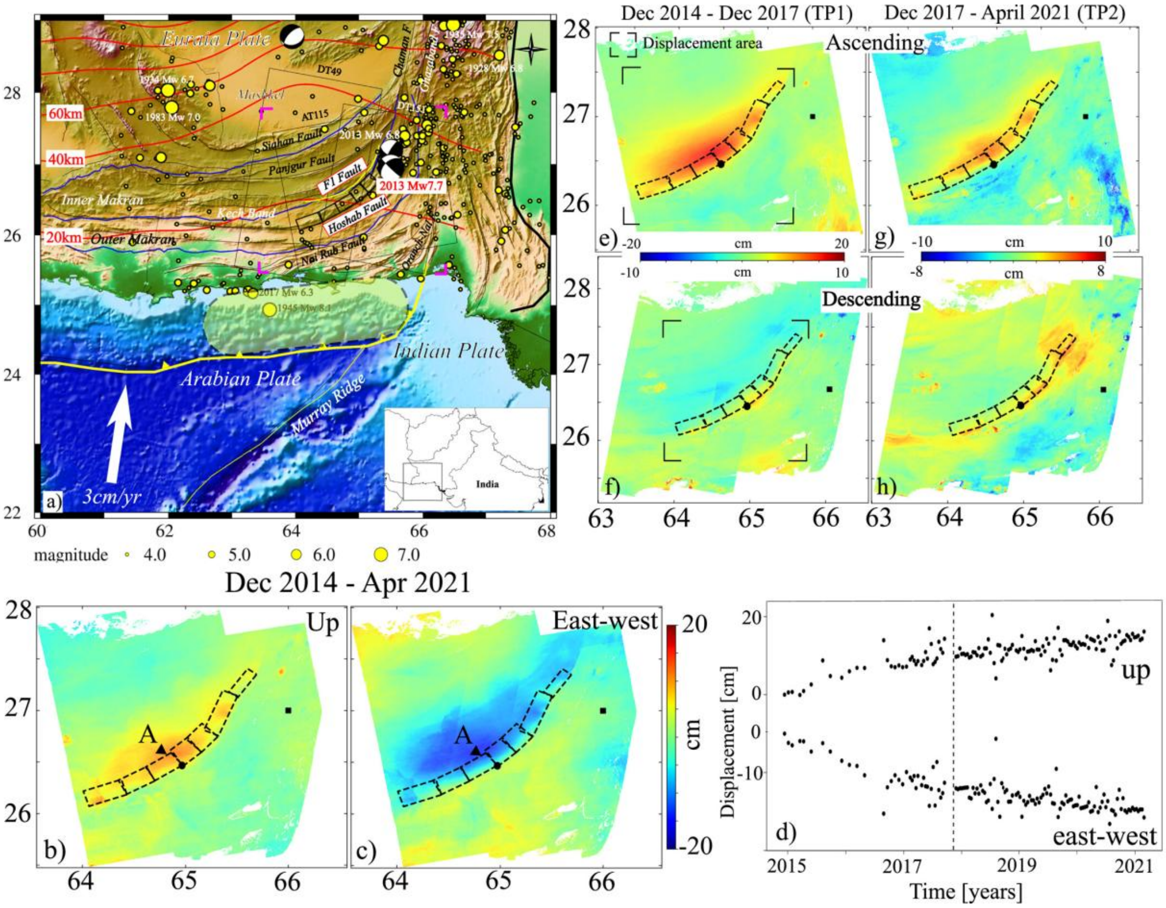

Figure 20. (a) Map of the study area with Sentinel-1 SAR coverage. Cumulative (b) up and (c) east-west displacement components and (d) time series for a point located in the epicentral area. (e–h) Ascending and descending line-of-sight displacements for time periods 1 and 2.

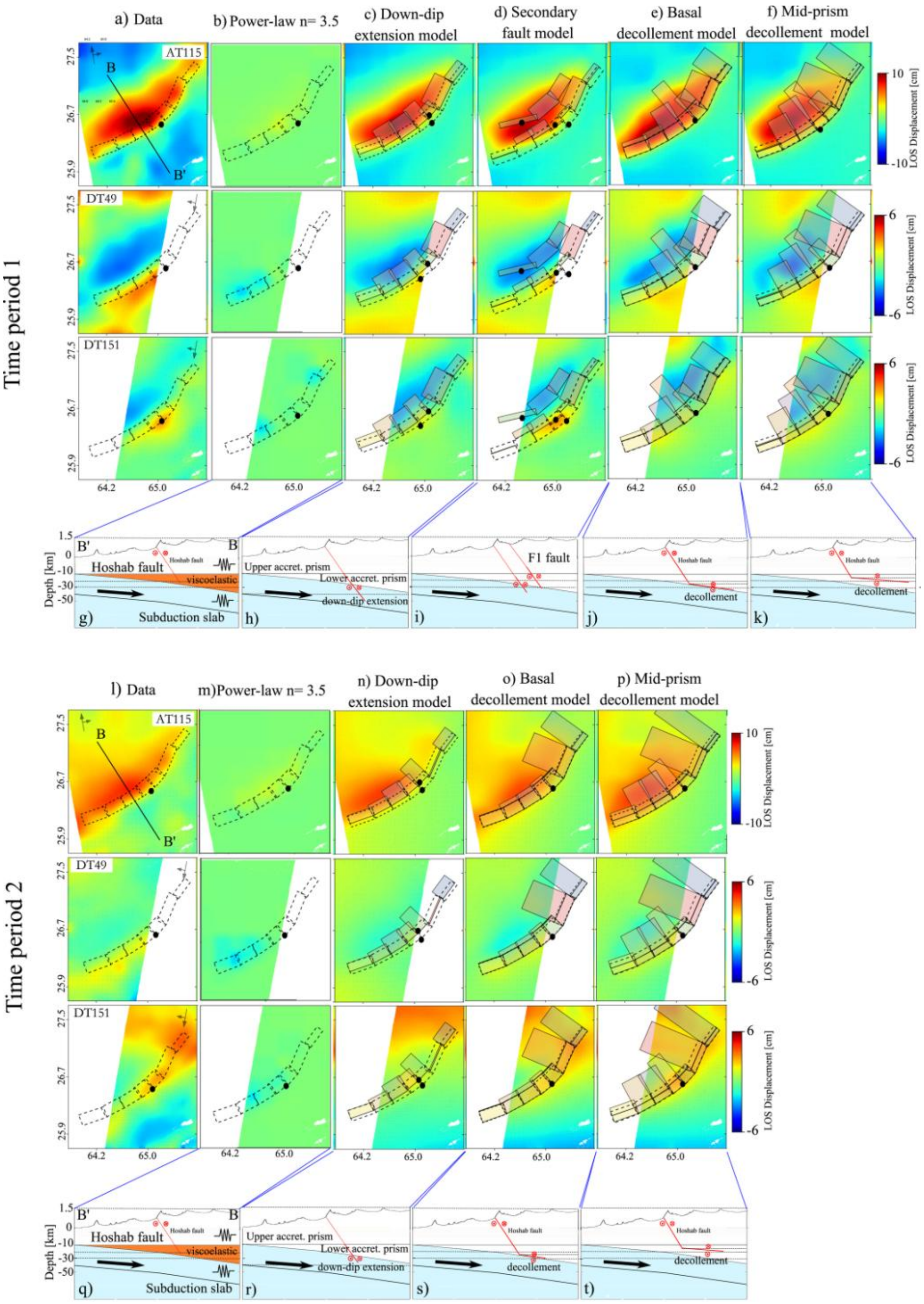

Figure 21. (a) Interpolated observed line-of-sight (LOS) displacements of time period 1. Modeled LOS displacements of time period 1 for (b) viscoelastic relaxation model, (c) down-dip extension model, (d) secondary fault model, (e) basal decollement model and (f) mid-prism decollement model. In (a–f): Black dashed rectangle: coseismic fault segments; black dot: upper edge of the fault; black solid rectangle: aseismic slip faults. Conceptual sketches along profile BB' for (g) relaxation model, (h) down-dip extension model, (i) secondary fault model (j) basal decollement model and (k) mid-prism decollement model. (l–t) same as (a–k) but for time period 2 and without secondary fault model.

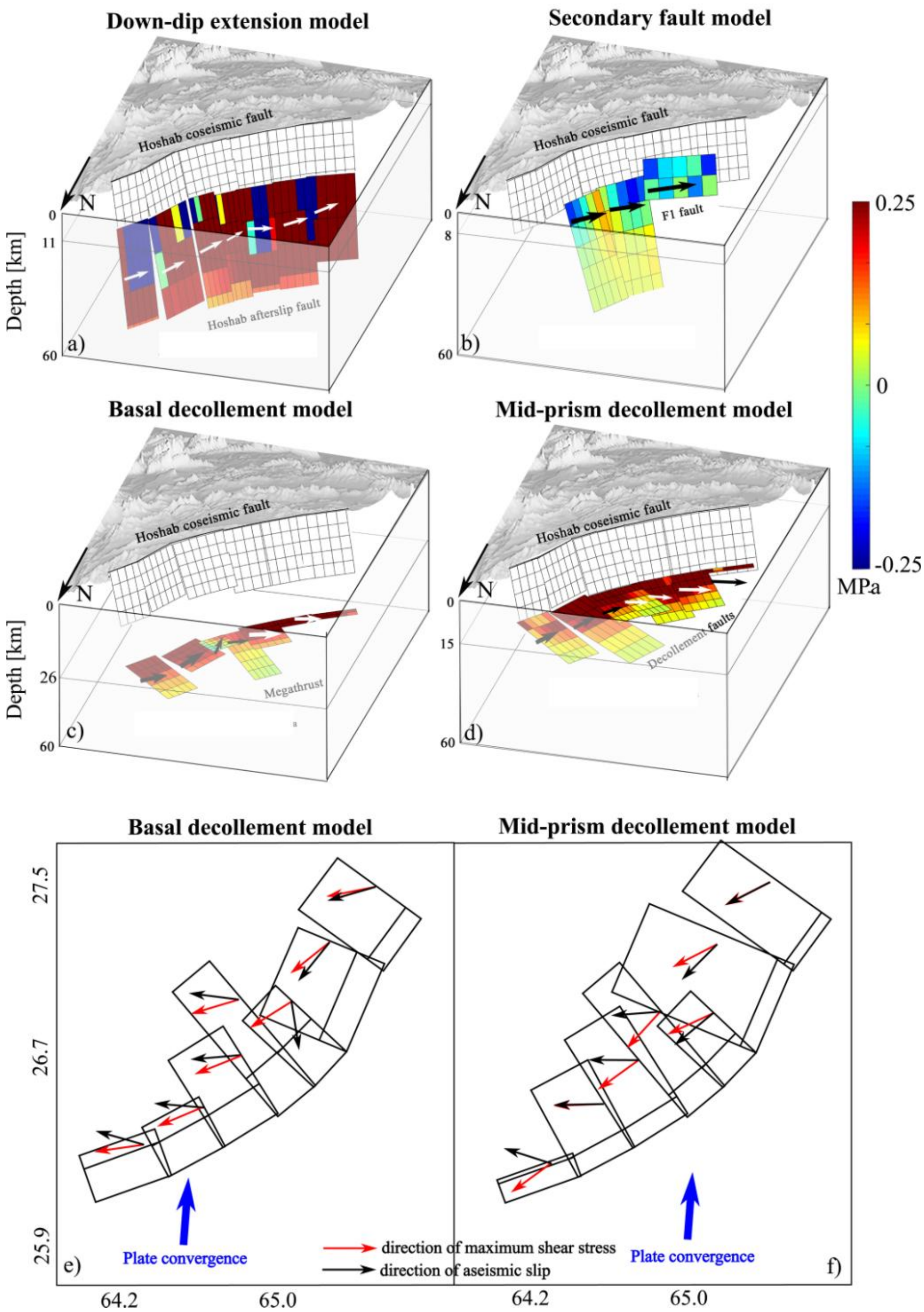

Figure 22. Coulomb stress changes in the direction of inferred slip along the aseismically sliping faults impart ed by the coseismic slip distribution: (a) down-dip extension model; (b) F1 fault, (c) basal decollement model, (d) mid-prism decollement model. Black and white arrows: slip direction of the overriding block along the dec ollement. Direction of maximum coseismic shear stress and aseismic slip for (e) basal decollement model, (f) mid-prism decollement model, using unit length for arrows.

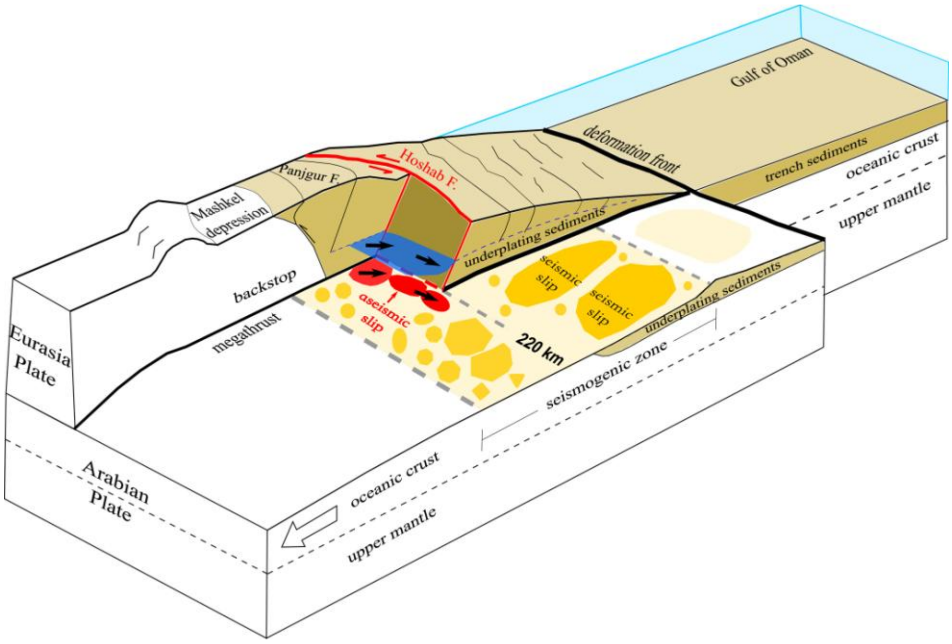

Figure 23. Schematic illustration of triggered aseismic slip (red patch) along the Makran megathrust. Blue pat ch and blue dashed line: alternate location of aseismic slip along mid-prism decollement fault above underpla ting sediments. Orange regions on megathrust: area of seismic slip; yellow regions: conditionally stable; whit e regions: aseismic slip.

Publications

Peer reviewed journal articles
[1] Xiaora Lv, Falk Amelung, Yun Shao*. Widespread Aseismic Slip Along the Makran Megathrust Triggered b y the 2013 Mw 7.7 Balochistan Earthquake. Geophysical Research Letters, 2022, 49(6), e2021GRL097411
[2] Xiaoran Lv, Yun Shao*. Rheology of the Northern Tibetan Plateau Lithosphere Inferred from the Post-Seis mic Deformation Resulting from the 2001 Mw 7.8 Kokoxili Earthquake. Remote Sensing. 2022, 14, 1207
[3]Xiaoyong Wu,Yun Shao,Ming Liu,et al. High-resolution strain partitioning along Haiyuan fault of northeast ern Tibetan Plateau from Sentinel-1 InSAR data. (Submitting)
[4] Xiaoyong Wu,Yun Shao,Ming Liu,et al. Shallow creep along Haiyuan fault through joint inversion of InSAR and GPS data. (in prep.)
Conference presentations/proceedings
Falk Amelung, Xiaoran Lv. Rheological structure of the East Asia lithosphere from InSAR observations of post-seismic deformation of large continental earthquakes. ACRS Keynote 2020.

Research products

Type of product	Product	How to access	Type of access

	provider		
ground deformation	Xiaoyong Wu,Yun Shao,Falk Amelung	We have processed the Sentinel1 time series satellite images of the past five years using the time-series InSAR technology, and obtained the velocity fields of Haiyuan fault and Longmenshan fault.	public
interseismic coupling model	Xiaoyong Wu,Yun Shao	We use screw dislocation model and block model to inverse the fault slip rate and interseismic coupling state of Haiyuan fault.	public
the InSAR velocity of Balochistan in Pakistan	Xiaoran Lv, Falk Amelung, & Yun Shao	https://doi.org/10.1029/2021GL097411	public

Research product issues

1) All our research results will be presented in the form of academic papers or reports, so anyon e who are interested in the research results can obtain them.

2) The research results need to be further improved. Our current work is far from the expected result, so it will be further improved in the future.

4. Dissemination and outreach

The ultimate objective of the Supersite is to facilitate open access to all Chinese GNSS and seismic data and data products following the GEO data sharing principles. Open data access to both data products and raw data exists in the U.S., Europe and Japan. In China, data access was historically restricted but policies are opening up. An important step forward is the new China S eismic Experimental Site (CSES) which will have open data access (see below).

Our strategy to advance open data access is (1) by demonstrating the benefits using the sa tellite data provided by the GSNL initiative, and (2) by defining and implementing new open dat a access milestones every 2 years when the Supersite is up for renewal. This proposal has two c o-PIs affiliated with the CEA (Prof. Wang and Prof. Qu), who have agreed to make the CEA leade rship aware of GEO's open data sharing policies.

Data sharing for ground acceleration recordings: Open access was provided to the ground acc eleration recordings of the 2008 Wenchuan earthquake at the occasion of the 2010 Beijing GE O plenary (network operated by the National Strong Earthquake Network Center https://www.i em.ac.cn/detail.html?id=1798 , These recordings are today available on request https://data.earthquake.cn/datashare/report.shtml?PAGEID=datasourcelist&dt=40280d0453e5add30153e5eae980001e

Data sharing at the CSES site: The China Seismic Experimental Site (CSES) (http://www.cses.ac.cn/) maintains an open data and collaboration policy and warmly welcome scientists from the international community to participate in studies. The CSES scientists will provide basic data and models of the region, including fault map, crustal velocity models, GPS velocity field, etc. During the first two years of the project the point-position timeseries for the CSES site (Longmenshan fault) and for the Haiyuan fault areas (base and regional data) will be placed on the CSES website.

5. Funding

Supersite objectives are supported by:

1) National Key Research and Development Program of China: Construction and Demonstration of Accurate Emergency Service System for aerial-space-ground based cooperative remote sensing.

2) Scientific Innovation Team Project: The study on Co-seismic and Post-seismic Deformation with InSAR technology.

6. Stakeholders interaction and societal benefits

Benefits for emergency management: Satellite-derived earthquake deformation data will aid emergency management department to respond to earthquakes.The study results about interseismic and postseismic deformation will be provided to the emergency management department, and we will try to place these results on CSES website (http://www.cses.ac.cn/).

7. Conclusive remarks and suggestions for improvement

This Supersite proposal has three scientific objectives and one data sharing objective : 1) Longmenshan Fault post-seismic deformation. Acquire Sentinel-1 imageries of the 2008 Wenchuan earthquake region in order to better resolve post-seismic deformation and understand how i t affects nearby faults. 2) Haiyuan Fault interseismic deformation. Acquire high-resolution Cosmo-Skymed imageries of a selected section of the Haiyuan fault to study aseismic creep. 3) Support the China Seismic Experimental Site (CSES). Acquire Sentinel-1 imagery at CSES sites to map the interseismic deformation. 4) Data sharing. Advance data sharing (e.g. GNSS, Seismic waveforms,et al) in China and promote international collaboration and participation of China in the GSNL initiative.

We have focused on a series of earthquakes with magnitudes greater than 7 in east Asia, including the 1920 Haiyuan Mw7.9 earthquake, the 1976 Tangshan Mw7.6 earthquake, the 2001 Kokoxili Mw7.8 earthquake, the 2008 Wenchuan Mw7.9 earthquake in China, and the 2013 Balochistan Mw7.7 earthquake in Pakistan, etc. Our results will contribute to understand mechanism of earthquake occurence and benefit to evaluate seismic hazard. But there is only a brief presentation of some of the research results. For more information, please refer to our published articles. In the future, we will continue to improve the geophysical models, and integrate the GPS velocity field with InSAR velocity field in order to improve the accuracy and precise of deformation observation and parameter eastimation.

8. Dissemination material for CEOS (discretionary)

References:

Fattahi H, & Amelung F. InSAR observations of strain accumulation and fault creep along the Chaman Fault system, Pakistan and Afghanistan[J]. Geophysical Research Letters, 2016, 43: 8399-8406.

Fattahi H, Agram P, & Simons M. A Network-Based Enhanced Spectral Diversity Approach for TOPS Time-Series Analysis[J]. IEEE Transactions on Geoscience and Remote Sensing 2017, 55: 777-786.

Lv X, Shao, Y. Rheology of the Northern Tibetan Plateau Lithosphere Inferred from the Post-Seismic Deformation Resulting from the 2001 Mw 7.8 Kokoxili Earthquake[J]. Remote Sensing, 2022, 14, 1207. https://doi.org/10.3390/rs14051207

Lv X, Amelung F, & Shao Y. Widespread aseismic slip along the Makran megathrust triggered by the 2013 Mw 7.7 Balochistan earthquake[J]. Geophysical Research Letters, 2022, 49, e2021GL097411. https://doi.org/10.1029/2021GL097411

Molnar P, and Tapponnier P. Cenozoic tectonics of Asia: Effects of a continental collision[J].Science,1975,189(4201):419–426.doi:10.1126/science.189.4201.419

Taylor M and Yi A. Active structures of the Himalayan-Tibetan orogen and their relationships to earthquake distribution, contemporary strain field, and Cenozoic volcanism[J]. Geosphere, 2009,5(3):199-214. doi:10.1130/GES00217.1

Yunjun Z, H Fattahi, & F Amelung. Small baseline InSAR time series analysis: Unwrapping error correction and noise reduction[J]. Computers&Geosciences, 2019,133, 104331.

Yin A, & Harrison T M. Geologic Evolution of the Himalayan-Tibetan Orogen[J]. Annual Review of Earth and Planetary Sciences, 2000,28(1):211–280. doi:10.1146/annurev.earth.28.1.211